Available online at www.sciencedirect.com
SCIENCE DIRECT®
Biochemical Pharmacology 68 (2004) 423–432
Biochemical Pharmacology
www.elsevier.com/locate/biochempharm

Prostaglandin H synthases: members of a class of quasi-linear threshold switches

William D. Hazelton[a,*], Joseph H. Tien[b], Vinsunt W. Donato[c], Rachel Sparks[a], Cornelia M. Ulrich[a]

[a]*Public Health Sciences Division, Fred Hutchinson Cancer Research Center, 1100 Fairview Avenue North, M2 B500 Seattle, WA 98109-1024, USA*
[b]*Center for Applied Mathematics, Cornell University, Ithaca, NY 14853, USA*
[c]*Whitman College, 345 Boyer Ave, Walla Walla, WA 99362, USA*

Received 19 November 2003; accepted 13 April 2004

Abstract

Prostaglandin H synthase (PTGS or COX) enzymes catalyze rate-limiting steps in the synthesis of potent prostanoids, including various prostaglandins, thromboxane, and prostacyclin. Mechanisms that have evolved for regulating prostanoid biosynthesis reflect a tension between achieving a rapid but measured response to cellular signals while minimizing spurious activation by signal noise. We found through mathematical modeling that the PTGS enzymes can be thought of as regulatory switches with approximately linear output above an adjustable threshold. In vivo synthesis allows continuous production while signal remains above threshold. Different isoforms show specific adaptions reflecting their physiological roles as constitutive or inducible enzymes. Mathematical modeling helps explain how these adaptations enable the PTGS1 and PTGS2 enzymes to maintain their physiological roles while avoiding potentially damaging consequences.

Keywords: PTGS1; PTGS2; COX1; COX2; Threshold switch; Noise rejection

1. Introduction

Prostaglandin H synthases (PTGS or COX, also known as prostaglandin endoperoxide G/H synthase or PGHS) combine two enzymatic activities, first a cyclooxygenase activity that converts arachidonic acid (or similar polyunsaturated fatty acids) to prostaglandin G_2 (PGG_2), a hydroperoxide intermediate, then a peroxidase activity that reduces PGG_2 to form prostaglandin H_2 (PGH_2). These two activities are linked to one another in an autocatalytic fashion: PTGS must first catalyze a peroxidase reaction before it can catalyze a cyclooxygenase reaction, and the product of the cyclooxygenase reaction serves as substrate for the peroxidase reaction [1]. Production of PGH_2 is the rate-limiting step in the production of numerous physiologically important prostaglandins, thromboxane, and prostacyclin. At least two different forms of PTGS exist, PTGS1 and PTGS2, which serve different functions in the body and thus present different regulatory challenges. These prostanoids mediate a number of important functions, including development, inflammation, blood clotting, pain, and tumorigenesis, yet questions remain about how these potent enzymes are regulated [2]. In this report, we show through mathematical modeling that the PTGS isozymes can be viewed as regulatory switches: there is a critical substrate (arachidonic acid) concentration at which PTGS activity becomes self-sustaining. Production of PGH_2 is much greater above compared with below the switch point. We first use a basic Michaelis–Menten-style model to derive an expression for the switch point. We then demonstrate that existing detailed models of PTGS kinetics [3,4] exhibit the same qualitative behavior as the basic model, show that the different isozymes of PTGS have different switch points appropriate to their biological functions, and examine ways to further tune PTGS activity by varying the glutathione peroxidase (GSP) concentration and PTGS synthesis rates.

Abbreviations: PTGS, prostaglandin H synthase; COX, prostaglandin H synthase; PGHS, prostaglandin H synthase; PGG_2, prostaglandin G_2; PGH_2, prostaglandin H_2; GSP, glutathione S peroxidase

* Corresponding author. Tel.: +1-206-667-7495; fax: +1-206-667-7004.
E-mail address: hazelton@fhcrc.org (W.D. Hazelton).

0006-2952/$ – see front matter © 2004 Elsevier Inc. All rights reserved.
doi:10.1016/j.bcp.2004.04.001

PTGS1 is constitutively expressed at stable levels in mammalian tissue, with an abundance of enzyme in a latent form, allowing synthesis of prostanoids within several minutes of stimulation for 'housekeeping' functions such as the regulation of homeostasis and protection of the gastric mucosa [2,5]. The inducible PTGS2 enzyme is generally absent or expressed at low levels under normal physiological conditions. Cytokines and mitogens rapidly induce PTGS2 mRNA transcription leading to high levels of protein expression, prolonging and enhancing inflammation and pain [6]. PTGS2 may suppress apoptosis, and its expression is often elevated in colon and other cancers [7,8].

The different PTGS isozymes utilize common substrates, incorporate similar coupled cyclooxygenase and peroxidase catalytic mechanisms, and produce identical PGG_2 hydroperoxide intermediate and PGH_2 product [2,9]. Regulation of PGH_2 production by PTGS enzymes depends on the substrate concentration, e.g. arachidonic acid or similar polyunsaturated fatty acids, and also on the availability of peroxide, including the hydroperoxide intermediate, PGG_2 [10]. Arachidonic acid levels are influenced by stimulus-induced action of phospholipase A_2 enzymes [9,11] that liberate arachidonic acid from membrane glycerophospholipids. Arachidonic acid also diffuses quite freely between compartments and across cell membranes [9,11]. Phospholipase A_2 activity can thus rapidly compensate for arachidonic acid consumption by PTGS, and we therefore expect the arachidonic acid concentration to change relatively slowly. In vivo peroxide levels reflect input from various sources, scavenging by efficient enzymes such as the glutathione peroxidases [12,13], along with production and consumption of PGG_2 by PTGS enzymes through their cyclooxygenase and peroxidase catalytic activities, respectively.

The regulatory challenge regarding the constitutively expressed PTGS1 is to avoid unwanted prostaglandin production and depletion of enzyme while substrate (arachidonic acid) is present at low concentrations in vivo. This is in contrast with the inducible PTGS2, for which a rapid response to stimuli is desired. Prostaglandin production can continue for hours or days in association with inflammation or pain, whereas PGH_2 synthesis in the laboratory ceases within minutes due to enzyme inactivation [14,15]. We consider all of these regulatory questions in connection with the 'switch' exhibited by both the basic and detailed kinetic models of PTGS that are discussed in the following sections.

2. Materials and methods

2.1. Basic model

We begin by presenting a simple extension of the Michaelis–Menten scheme to an autocatalytic enzyme such as PTGS, as shown in Fig. 1. In the Michaelis–Menten scheme, enzyme binds reversibly to substrate to form an enzyme–substrate complex. This enzyme–substrate complex, also called a Michaelis complex, is then converted to product. Free enzyme is also liberated in this last step. For extending the Michaelis–Menten scheme to PTGS, we define the variables as shown in Table 1.

The reaction scheme is:

$$E + P \overset{k_a,k_b}{\Leftrightarrow} C \overset{k_c}{\rightarrow} E^* + P' \quad (1)$$

$$E^* + S \overset{k_d,k_e}{\Leftrightarrow} C^* \overset{k_f}{\rightarrow} E^* + P \quad (2)$$

$$E^* \overset{k_g}{\rightarrow} E \quad (3)$$

$$E^* \overset{k_h}{\rightarrow} E_{\text{inact}} \quad (4)$$

The peroxidase and cyclooxygenase activities of PTGS are given by Michaelis–Menten-like reactions (1)–(2), modified to reflect the autocatalytic activity of PTGS. Reaction (3) allows for PTGS to go from the cyclooxygenase state to the peroxidase state. Reaction (4) incorporates enzyme inactivation, also called suicide inactivation

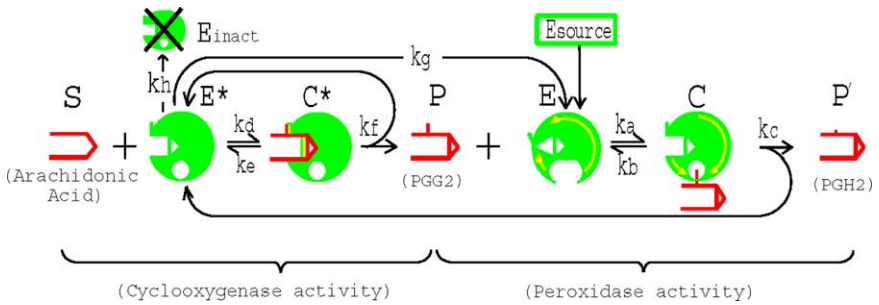

Fig. 1. Basic model. To start the reaction, a small amount of intermediate product P must be introduced. When viewed as a simplified representation for PTGS enzyme activity, P represents PGG_2 hydroperoxide that interacts reversibly with latent PTGS enzyme E through its peroxidase activity to form complex C. C can decay to form activated enzyme (E^*) and final product (P') representing PGH_2. E^* can decay to latent enzyme E or become inactivated. Substrate S (arachidonic acid) interacts reversibly with activated enzyme E^*, adding two oxygen atoms through its cyclooxygenase activity to form activated complex C^*. C decays to intermediate product and P (PGG_2) and E^*. The peroxidase and cyclooxygenase loops are decoupled, with cyclooxygenase producing PGG_2 (P) and peroxidase using it up to produce PGH_2 (P').

Table 1
Basic model parameters

E	Enzyme with peroxidase activity
C	Michaelis complex for peroxidase reaction
S	Arachidonic acid (substrate)
P'	PGH_2
E^*	Enzyme with cyclooxygenase activity
C^*	Michaelis complex for cyclooxygenase reaction
P	PGG_2
E_{inact}	Inert (suicide-inactivated) enzyme
k_a, k_b, k_c	Reaction rates for peroxidase reaction
k_d, k_e, k_f	Reaction rates for cyclooxygenase reaction
k_g	Transition rate from cyclooxygenase to peroxidase state
k_h	Suicide inactivation rate

[15]. Analogously to the original Michaelis–Menten scheme, define

$$K_m = \frac{k_b + k_c}{k_a}, \quad \hat{K}_m = \frac{k_e + k_f}{k_d}.$$

K_m can be thought of as the Michaelis constant for the peroxidase reaction, and $\hat{K}_m$ the Michaelis constant for the cyclooxygenase reaction.

The corresponding system of ODEs for the basic auto-catalytic model is:

$$\frac{dE}{dt} = k_b C + k_g E^* - k_a EP \tag{5}$$

$$\frac{dE^*}{dt} = k_c C + (k_e + k_f)C^* - E^*(k_d S + k_g + k_h) \tag{6}$$

$$\frac{dC}{dt} = k_a EP - (k_b + k_c)C \tag{7}$$

$$\frac{dC^*}{dt} = k_d E^* S - (k_e + k_f)C^* \tag{8}$$

$$\frac{dP}{dt} = k_f C^* + k_b C - k_a EP \tag{9}$$

$$\frac{dP'}{dt} = k_c C \tag{10}$$

$$\frac{dS}{dt} = k_e C^* - k_d(E^* S) \tag{11}$$

2.2. Numerics for the basic model

Simulations were done to assess the global behavior of the basic auto-catalytic model by systematically generating random parameter values, numerically solving the ODEs, and examining the behavior. Parameter values were selected from a uniform distribution on [0, a_p], where a_p varies for different parameters. To determine the value of a_p, we first note that we are considering ODEs of the form:

$$\dot{x}_i = \sum_{j,r} k_j x_{r_j} + \sum_{l,s,t} k_l x_{s_l} x_{t_l}$$

The first sum includes unimolecular reactions, and the second term gives bimolecular reactions. On physical grounds, there should be some upper bound $\mathscr{D}$ such that $|\dot{x}_i| < \mathscr{D}$. If we thus select parameter values so that each term on the right hand side of the $\dot{x}_i$ equation is less than $\mathscr{D}$, we will ensure that all physically feasible parameter values are included in our sampling regime.

Consider a typical bimolecular term $k_a EP$. Let E_m, P_m be the maximum concentrations of enzyme and peroxide that are physiologically possible. To ensure that $k_a EP < \mathscr{D}$, it suffices to choose $k_a < \mathscr{D}/(E_m P_m)$. So $a_{k_a} = \mathscr{D}/E_m P_m$ in our uniform distribution.

The numerical value of a depends upon the units in which we measure concentration and time. We choose to measure concentration in units of E_m. As a rough guess from in vitro experiments, we estimate that $(P_m/E_m), (S_m/E_m), (I_m/E_m) = 10^4$. Finally, note that we can then choose time units so that $\mathscr{D}$ has any numerical value we wish. The majority of our simulations were done with $\mathscr{D} = 10^4$.

The simulations were done in Matlab using the stiff solvers ode15s and ode23s. The relative tolerance was set to 10^{-8}, and the absolute tolerance was 10^{-12}.

2.3. Branched chain model

Two different types of models of PTGS kinetics have been proposed, the branched chain [3,4,16,17] and tightly coupled mechanisms [3,18]. We used the branched chain models here because the quantitative and qualitative predictions of the branched chain mechanism are largely consistent [3] with the observed characteristics of the PTGS reaction with arachidonic acid, but the observed characteristics are inconsistent with some predictions of the tightly coupled mechanism [3]. Several variations of the branched chain mechanism have been proposed [1,3,4,17–24], differing primarily by including two [17,24], one [22] or no [4,19] intermediates in the cyclooxygenase loop, and by addition of enzyme intermediates to allow continued peroxidase activity at the heme site after formation of the tyrosyl radical in the cyclooxygenase site [4,19]. In the case of two intermediates in the cyclooxygenase loop, two O_2's have been proposed to be added to generate the second intermediate [17,23,24], or one O_2 added before and one after formation of the second intermediate [3], as illustrated in Fig. 2.

For the simulations reported here, we used Scheme 1 of Lu et al. [4], with the addition of a source term for the enzyme and GSP scavenging. We used rates from Lu et al. [4] appropriate to the Scheme 1 model for PTGS1 and PTGS2 determined through stopped flow spectrophotometric measurements of intermediate lifetimes at 4 °C, using several hydroperoxides as substrates. The state variables and parameters we used are shown in Table 2. We assumed a range of constant arachidonic acid concentrations and different ratios of GSP scavenging to total PTGS enzyme to approximate a range of intracellular conditions. We compared these results against two other branched

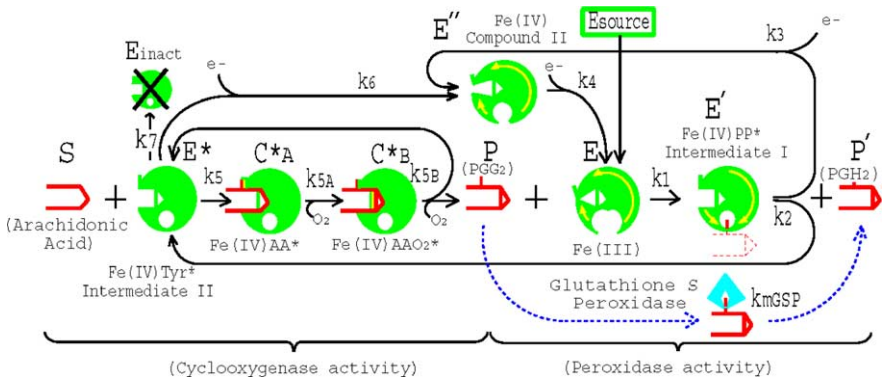

Fig. 2. Branched-chain PTGS model. This figure is adapted from Lu et al. [4], Tsai et al. [22], and Wei et al. [3], with addition of an enzyme source term and a pathway for scavenging of peroxide by glutathione peroxidase (GSP). This reaction scheme is similar to the basic model shown in Fig.1, but differs by including an intermediate (Fe(IV), Compound II) in the peroxidase loop, and intermediates C_A^* and C_B^* in the cyclooxygenase loop. Although the aggregate rate of the cyclooxygenase cycle can be estimated from measurements of the specific activity [4], individual rate constants k_5, k_{5A}, and k_{5B} are currently unavailable. Thus we modeled several variations of the reaction scheme. The results we present are based on a single rate to represent the rate-limiting step in the cyclooxygenase reaction using published rates appropriate for PTGS1 and PTGS2 [4]. We compared this to reaction schemes with insertion of two intermediates C_A^* and C_B^* using limiting values of estimates for k_{5A} and k_{5B} from Wei et al. [3]. Inclusion of one or both intermediates made no observable difference in the kinetics, with all systems showing nearly identical switching behavior depending on arachidonic acid and GSP concentrations, and the enzyme synthesis rate.

chain models by running simulations using (the more complicated) Scheme 2 of Lu et al. [4], and Scheme 1 from Wei et al. [3] (using the rate constants appropriate for PTGS1 in that manuscript). We found good agreement in the switching behavior of the three different schemes we tested.

The system of ODEs is:

$$\frac{dE(t)}{dt} = -k_1E(t)P(t) + k_4\mathrm{AH}(t)E''(t) + E_{\mathrm{source}}(t),$$
$$\frac{dE'(t)}{dt} = k_1P(t)E(t) - k_3\mathrm{AH}(t)E'(t) - k_2E'(t),$$
$$\frac{dE''(t)}{dt} = k_3\mathrm{AH}(t)E'(t) - k_4\mathrm{AH}(t)E''(t) + k_6\mathrm{AH}(t)E^*(t),$$
$$\frac{dE^*(t)}{dt} = -k_6\mathrm{AH}(t)E^*(t) - k_7E^*(t) + k_2E'(t),$$
$$\frac{dE_{\mathrm{inact}}(t)}{dt} = k_7E^*(t), \quad \frac{d\mathrm{AA}(t)}{dt} = 0,$$
$$\frac{dP(t)}{dt} = \left(\frac{k_5E^*(t)}{1 + K_{\mathrm{mAA}}/\mathrm{AA}(t)}\right) - k_1P(t)E(t) - \left(\frac{R_{\mathrm{GC}}K_5(E_{\mathrm{total}})}{1 + K_{\mathrm{mGSP}}/P(t)}\right), \quad \frac{dP'(t)}{dt} = k_1P(t)E(t) + \frac{R_{\mathrm{GC}}K_5(E_{\mathrm{total}})}{1 + K_{\mathrm{mGSP}}/P(t)}, \quad \frac{d\mathrm{AH}(t)}{dt} = -k_3\mathrm{AH}(t)E'(t) - k_4\mathrm{AH}(t)E''(t) - k_6\mathrm{AH}(t)E^*(t). \tag{12}$$

R_{GC} determined the ratio of GSP to total PTGS enzyme. Simulations were done using Matlab and Mathematica.

3. Results

Our main result is that there exists a threshold arachidonic acid concentration at which the PTGS reaction became self-sustaining. This 'switch point' was found in both the basic model, and in the branched chain model. We first carried out a local stability analysis in the basic model to derive an expression for the switch point. The switch point also appeared under the quasi-steady-state approximation (QSSA), which is typically made in these types of models. We then examined the global behavior of the basic model through numerical simulations, and observed the qualitatively different behaviors above and below the switch point. Finally, we found through numerical simulations that the branched chain models also exhibit this switching behavior, and examined how this switch point varied between the different PTGS isozymes and under different physiological conditions.

3.1. Basic model results

3.1.1. Local stability

We examined the local stability of fixed points of the basic model for PTGS under the assumptions that suicide inactivation is absent ($k_h = 0$) and arachidonic acid concentration S is held constant. In the section on the global behavior of the system, we discuss the behavior when these assumptions are relaxed.

We ordered the variables in system (5)–(11) as (E, E^*, C, C^*, P, P', S). Fixed points occur either when peroxide is absent (E, 0, 0, 0, 0, P', S), or when enzyme is absent (0, 0, 0, 0, P, P', S). Let $E_0 = E(0) + E^*(0) + C(0) + C^*(0)$, where the notation reflects that $E_0 = E(0)$ is the initial condition of greatest interest. Under the assumption $k_h = 0$, we have the conservation law $E_0 = E(t) + E^*(t) + C(t) + C^*(t)$ for all times t. We eliminated E from the system by setting $E = E_0 - E^* - C - C^*$. Note that P' does not appear on the right hand sides of the equations for any of the variables, and thus plays no role in determining

Table 2
Branched chain model parameters and reaction rates for PTGS1 and PTGS2

Parameters	Alternate names, reaction steps	PTGS1 initial values	PTGS2 initial values	Units
E	Fe(III), resting enzyme	0.01	0.01	μM
E'	Fe(IV)PP*, intermediate I	0	0	μM
E''	Fe(IV), compound II	0	0	μM
P'	PGH_2, ROH	0	0	μM
S	Arachidonic acid, AA	0–100‡	0–100‡	μM
E^*	Fe(IV)Tyr*, intermediate II	0	0	μM
C_A^{*} ‡	Fe(IV)AA*	0	0	μM
C_B^{*} ‡	Fe(IV)AAO_2^*	0	0	μM
P	PGG_2, ROOH	0.001	0.001	μM
e^-	AH, reducing cosubstrate	100	100	μM
E_{inact}	Inactivated enzyme	0	0	μM
k_1	$E + P \rightarrow E' + P'$	100	100	$(\mu M)^{-1}\ s^{-1}$
k_2	$E' \rightarrow E^*$	350	2000	s^{-1}
k_3	$E' + AH \rightarrow E'' + AH^*$	0.4	0.4	$(\mu M)^{-1}\ s^{-1}$
k_4	$E'' + AH \rightarrow E + AH^*$	0.4	0.4	$(\mu M)^{-1}\ s^{-1}$
k_5†	$C_A^* + S \rightarrow C_A^*$	1	1	$(\mu M)^{-1}\ s^{-1}$
k_{5A}†	$C_A^* + O_2 \rightarrow C_B^*$	≥5.0	≥5.0	$(\mu M)^{-1}\ s^{-1}$
k_{5B}†	$C_B^* + O_2 \rightarrow C^*P$	≥5.0	≥5.0	$(\mu M)^{-1}\ s^{-1}$
k_5‡	$E^* + S \rightarrow E^* + P$	60	60	s^{-1}
k_{mAA}‡	K_m value for S (AA)	3	3	M
k_6	$E^* + AH \rightarrow E'' + AH^*$	0.004	0.00025	$(\mu M)^{-1}\ s^{-1}$
k_7	$E^* \rightarrow E_{inact}$	0.06	0.06	s^{-1}
R_{GC}	Ratio of GSP to enzyme	0–600	0–600	
k_{mGSP}	K_m value for GSP	1.5	1.5	M

Parameters for Scheme 1 of Wei et al. [3] (including two intermediates in the cyclooxygenase loop) are indicated by the symbol †; and model parameters and reaction steps based on Scheme 1 of Lu et al. [4] are shown by ††. The remaining parameters are common to all the branched chain models we tested. The arachidonic acid (S) concentration ‡ was assumed to be held constant at different levels for each simulation, with R_{GC} determining the ratio of GSP to total PTGS enzyme.

the stability of the fixed points. Ignoring the P' dynamics and treating S as a fixed parameter leaves a four dimensional vector field with variables (E^*, C, C^*, P).

The fixed points are of the form (0, 0, 0, P), with $P > 0$ possible only when $E_0 = 0$. The conservation law implies that fixed points having $P > 0$ are destroyed by perturbations to $E_0 > 0$. We thus need only determine the stability of (0, 0, 0, 0).

The characteristic polynomial of the Jacobian at 0 is given by

$$p(\lambda) = \lambda^4 + a_1\lambda^3 + a_2\lambda^2 + a_3\lambda + a_4,$$

where

$$a_1 = k_a E_0 + k_b + k_c + k_d S + k_e + k_f + k_g,$$
$$a_2 = k_d S(k_b + k_a E_0 + k_c) + k_a E_0(k_c + k_e + k_f + k_g) + (k_e + k_f + k_g)(k_b + k_c) + k_g(k_e + k_f),$$
$$a_3 = k_f k_g(k_a E_0 + k_b + k_c)k_a E_0(k_e(k_c + k_g) + k_c(k_d S + k_f + k_g)) + k_e k_g(k_b + k_c),$$
$$a_4 = k_a E_0 k_c((k_e + k_f)k_g - k_d k_f S).$$

By the Routh–Hurwitz criterion, all roots of p have negative real part if and only if (i) $a_1, a_3, a_4 > 0$, and (ii) $a_1 a_2 a_3 > a_3^2 + a_1^2 a_4$ [25]. As $E_0 >= 0$ and all the rate constants k_i are positive, we have a_1, $a_3 > 0$. Similarly, direct computation gives that $a_1 a_2 a_3 - a_3^2 - a_1^2 a_4$ is comprised only of sums of positive quantities. Thus the condition $a_1 a_2 a_3 > a_3^2 + a_1^2 a_4$ is always satisfied, and the stability of 0 is governed solely by the sign of a_4. From the expression for a_4, we have

$$a_4 > 0 \Leftrightarrow \frac{k_f S}{k_g \hat{K}_m} - 1 < 0.$$

Define

$$\sigma = \frac{k_f S}{k_g \hat{K}_m} - 1. \tag{13}$$

The stability at 0 is thus determined by σ, with $\sigma < 0$ corresponding to a stable fixed point and $\sigma > 0$ corresponding to instability. Phrased in terms of the arachidonic acid concentration S, we have a threshold value $S_{thresh} = (\hat{K}_m k_g / k_f)$at which the stability of the fixed point changes. This threshold value thus defines a switch point at which the PTGS activity changes qualitatively. Note that the switch point is independent of the rate constants associated with the peroxidase activity of PTGS.

3.1.2. Quasi-steady-state assumption

In the classical Michaelis–Menten scheme, a quasi-steady-state assumption (QSSA) is typically made, where the enzyme–substrate complex evolves on a fast time scale and substrate evolves on a slow time scale. The physical intuition behind the QSSA is discussed in biochemistry textbooks (e.g. [26]), and has been examined from a more mathematical viewpoint by Segel and Slemrod [27].

Consider the case where suicide inactivation is absent. Assume that E, E^*, C, C^* are the fast variables and P, P', S the slow variables. The QSSA consists of assuming that the right hand sides of the fast equations are equal to zero. We can then solve for the fast variables in terms of the slow variables. This solution set is called the *critical manifold*. When the separation of time scales is large, the flow of the slow variables on the critical manifold will in general be a good approximation to the flow of the actual system.

The initial condition of greatest interest is of the form $(E_0, 0, 0, 0, P_0, 0, S_0)$. In the absence of suicide inactivation, $E(t) + E^*(t) + C(t) + C^*(t) = E_0$ for all t. Thus we can eliminate the variable E from consideration. Solving for the critical manifold, we obtained:

$$E^* = \frac{k_c}{k_g} C, \tag{14}$$

$$C^* = \frac{k_c S}{k_g \hat{K}_m} C, \tag{15}$$

$$E = E_0 - C\left(\frac{k_c}{k_g}\left(1 + \frac{S}{\hat{K}_m}\right) + 1\right), \tag{16}$$

$$C = \frac{E_0 P}{(P(k_c/k_g)(1 + (S/\hat{K}_m)) + 1) + K_m}, \tag{17}$$

If we then look at dP/dt on the critical manifold, we have

$$\frac{dP}{dt} = \frac{k_c E_0 P \sigma}{P((k_c/k_g)(1 + (S/\hat{K}_m) + 1)) + K_m}, \tag{18}$$

where σ as defined in (13). Thus the sign of σ is the same as the sign of dP/dt on the critical manifold. This finding gives insight into the cause of the change in stability when $\sigma = 0$. Eq. (18) hints that the switch point occurs when P is produced faster than it is consumed, thus allowing the reaction to become self-sustaining. This intuition is supported by the numerical simulations described in the next section.

3.1.3. Global behavior

Extensive numerical simulations illustrate the global behavior associated with the switch point. Below the switch point ($S < (\hat{K}_m k_g/k_f)$, corresponding to $\sigma < 0$), peroxide P is consumed faster than it is produced and the reaction comes to a halt. Above the switch point $S > (\hat{K}_m k_g/k_f)$, corresponding to $\sigma > 0$), peroxide is produced faster than it is consumed, and the reaction continues indefinitely when S is held constant and suicide inactivation is absent.

3.1.4. Constant S and suicide inactivation absent

For the case where S is held constant and suicide inactivation is absent, we performed 10^6 simulations each for $S > (\hat{K}_m k_g/k_f)$ and $S < (\hat{K}_m k_g/k_f)$ using randomly generated parameter values selected from uniform distributions $[0, a_p]$. The value of a_p was chosen appropriately for different parameters based on the type of interaction (uni-molecular or bi-molecular) and plausible ranges for solubility ratios (details in Section 2).

In each simulation, we found that $S > (\hat{K}_m k_g/k_f)$ corresponds to unbounded production of peroxide and PGH_2, while $S < (\hat{K}_m k_g/k_f)$ corresponds to an eventual halting of the reaction. Fig. 3a and b compare two different trajectories of system (5)–(11), one with $S > (\hat{K}_m k_g/k_f)$ and the other with $S < (\hat{K}_m k_g/k_f)$. Note that in the $S > (\hat{K}_m k_g/k_f)$ case, dP/dt and dP'/dt eventually appear nearly constant and growth of P and P' is approximately linear with time. 250,000 simulations with $S = (\hat{K}_m k_g/k_f)$ illustrate that the switch point corresponds to a change in sign of net production of peroxide P: for each simulation with S exactly equal to the threshold value, production and consumption of peroxide eventually became exactly balanced and peroxide concentration approached a constant (positive) value.

3.1.5. Synthesis and inactivation of enzyme

Simulations indicated that a switch point persists when suicide inactivation and synthesis of enzyme are both present (i.e. $k_8 > 0$, $E_{source} > 0$). The numerical value of S corresponding to the switch point generally differs from the $k_8 = 0$, $E_{source} = 0$ case.

3.1.6. Behavior when S is allowed to vary

The behavior above and below the switch point when S was assumed constant provided a qualitative indication of the behavior when this assumption was relaxed. While S was greater than the threshold value $\hat{K}_m k_g/k_f$, we found that generally P was produced faster than it was consumed. When S fell below this threshold value, P was consumed faster than it was produced, and PTGS activity eventually halted.

3.2. Branched chain model results

We tested several branched-chain reaction mechanisms for PTGS1 and PTGS2 (Schemes 1 and 2 of Lu et al. [4], and scheme I of Wei et al. [3]) with similar topologies to that of the basic model (compare Figs. 1 and 2), differing only by the presence or absence of short-lived intermediates. Fig. 4 shows our results for the branched chain model based on Scheme 1 of Lu et al. [4], with switching for PTGS1 and PTGS2 that depends both on arachidonic acid concentration and on the level of scavenging by GSP. The results were consistent across all schemes we tested. Thus we found that these larger, branched chain networks for PTGS enzymes also have the switching property found in the basic model. Indeed, we expect this switching behavior to be manifest by any reaction that is well modeled by the extended Michaelis–Menten reaction scheme for an autocatalytic enzyme, as defined by the basic model reactions (5)–(11).

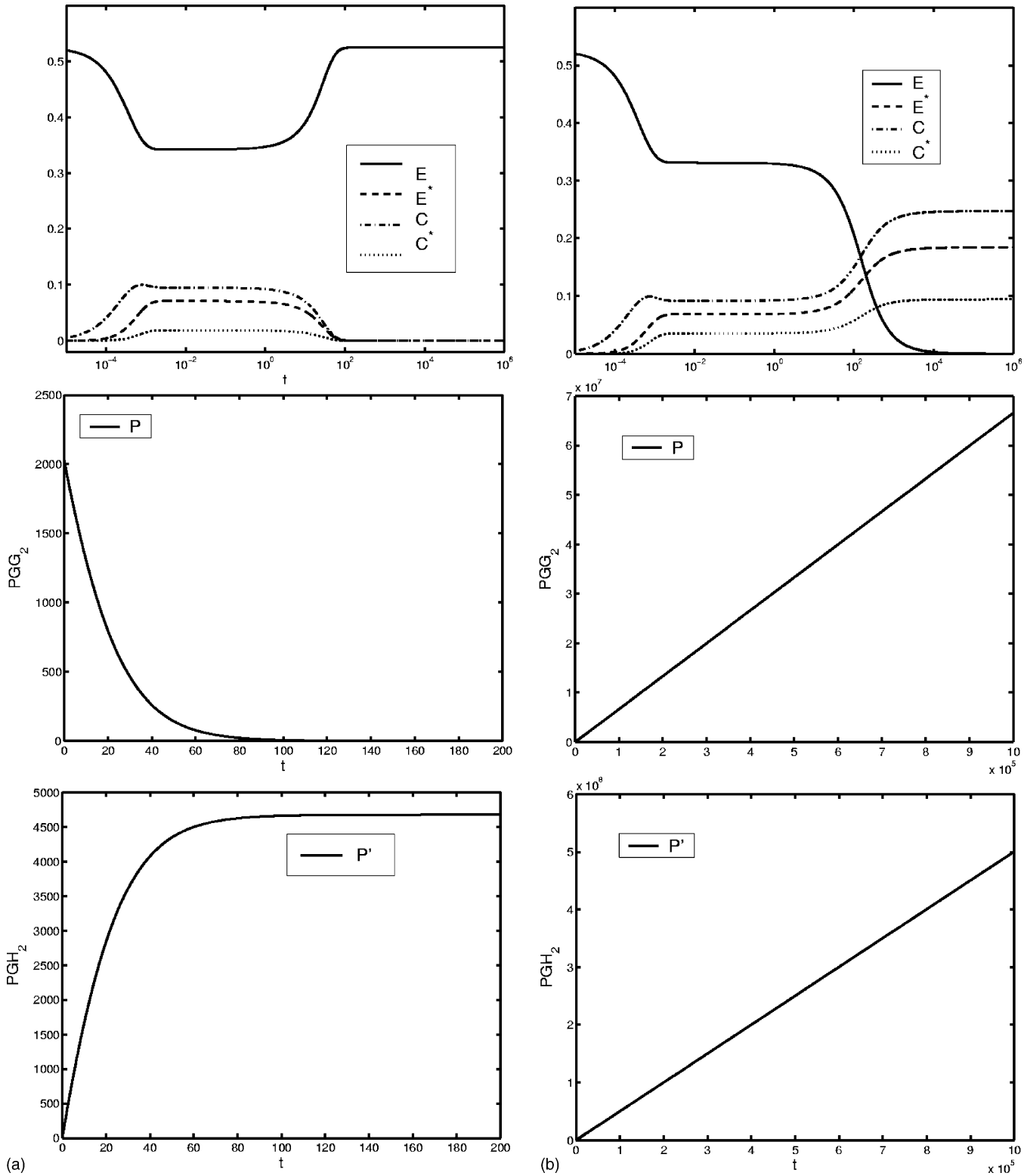

Fig. 3. Basic model enzyme kinetics system (5)–(10), with arachidonic acid concentration S held constant) below and above threshold. Column (a) depicts a typical trajectory for $\sigma < 0$, and column (b) a trajectory for $\sigma > 0$. Note the different time scale in the first row of plots compared with in the lower two rows. Parameter values are the same for (a) and (b), but the arachidonic acid concentration S in (a) is half that in (b). As seen in (a), when $\sigma < 0$ peroxide P is consumed faster than it is produced. The reaction comes to a halt when peroxide is completely consumed. (b) The reaction is sustained indefinitely, with production of P and P' becoming nearly linear in this case. As P increases, E decreases to maintain an approximately constant production rate of P. (The units are arbitrary.)

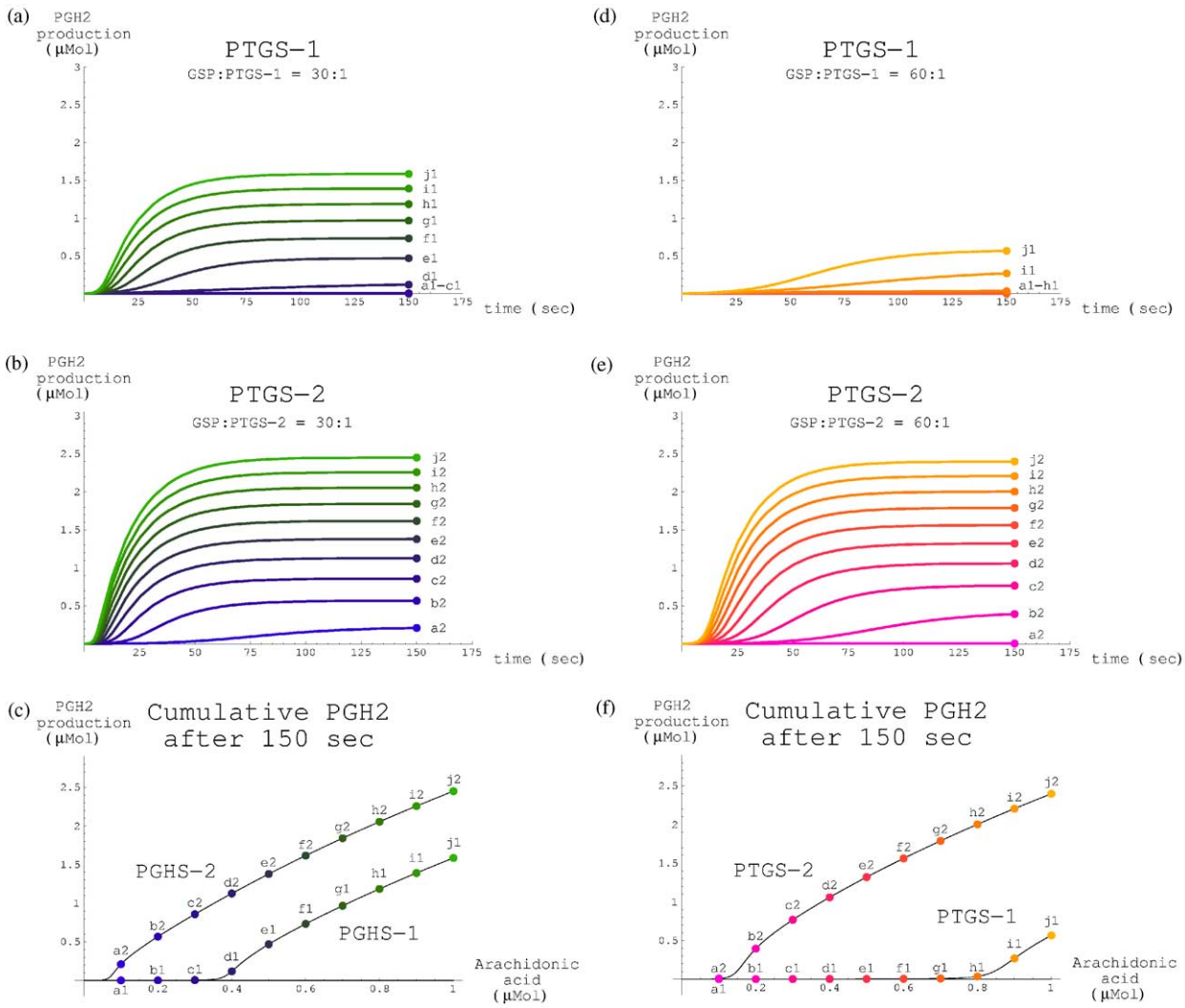

Fig. 4. Switching behavior for the branched chain PTGS1 and PTGS2 models. These simulations are based on Scheme 1 of Lu et al. [4]. The switching threshold depends both on the arachidonic acid and GSP concentrations. The plots show the cumulative production of PGH_2 based on the branched-chain model using parameters measured for PTGS1 and PTGS2 in the presence of different amounts of GSP peroxide scavenger. The series of lines in each figure, labeled a1–j1 for PTGS1 or a2–j2 for PTGS2, represent constant arachidonic acid concentrations ranging from 0.1 to 1.0 μM (in increments of 0.1 μM), respectively. (a) With 30 times as much GSP as enzyme, PTGS1 switches from minimal PGH_2 production for arachidonic acid levels below about 0.35 μM concentration, to nearly linear growth in PGH_2 production above this threshold. (b) PTGS2 switches at around 0.05 μM arachidonic acid concentration. (c) Cumulative production of PGH_2 at 150 s from (a–b) shows a higher switching threshold for PTGS1 than for PTGS2. PTGS1 and PTGS2 switch at higher levels with higher relative concentrations of GSP. (d–f) Switching of PTGS1 and PTGS2 with 60 times as much GSP as enzyme. The switching threshold for PTGS1 is increased to around 0.8 μM arachidonic acid, and the switching threshold for PTGS2 is increased to about 0.1 μM arachidonic acid.

In each of the branched-chain models, there was both production and consumption of the essential intermediate PGG_2, giving rise to a threshold switch. The reaction stopped if PGG_2 was depleted. The threshold for switching was determined by the amounts of arachidonic acid and glutathione peroxidase (GSP) that influenced the balance between production and consumption of PGG_2. Increasing the amount of arachidonic acid increased the rate of PGG_2 synthesis. Increasing the amount of GSP increased the rate of PGG_2 depletion, raising the threshold for switching.

This behavior is shown in Fig. 4 using the Scheme 1 branched chain model of Lu et al. [4], with the addition of a source term for enzyme and scavenging of peroxide by GSP, as defined in Eq. (12). Fig. 4a and b shows the cumulative production of PGH_2 as a function of time by PTGS1 and PTGS2, respectively, for a GSP:PTGS ratio of 30:1. Fig 4d and e are similar, except for a GSP:PTGS ratio of 60:1. PTGS1 switched at a higher arachidonic acid concentration than PTGS2. Both switch points increased as the GSP:PTGS ratio increased. Fig. 4c and f shows the total amount of PGH_2 produced at the end of 150 s by PTGS1 and PTGS2 as a function of the arachidonic acid concentration with GSP:PTGS ratios of 30:1 and 60:1, respectively. We found that the cumulative PGH_2 production is approximately a linear function of the arachidonic acid concentration above the switching threshold.

In Fig. 4 (with E_{source} set to zero) suicide inactivation essentially halted all of the reactions within 150 seconds.

When E_{source} was set greater than zero for an extended time interval, we found that PGH_2 production continued indefinitely while E_{source} remained above zero and the GSP and arachidonic acid concentrations were maintained such that the switch was on (not shown). This is consistent with the known behavior of the PTGS-mediated inflammatory response that can persist in vivo for hours or days. We found that the rate of steady-state PGH_2 production increased under each of the following conditions: the rate of enzyme synthesis was increased (modeled by using a higher value of E_{source}), the arachidonic acid level was increased further above the switching threshold, or the GSP:PTGS ratio was decreased to lower the switching threshold. (In the absence of GSP, the threshold remained above zero, while continuing to differ significantly between PTGS1 and PTGS2.)

The primary new result of the modeling reported here is that both the PTGS1 and PTGS2 enzymes behave as threshold switches, with thresholds that depend on intracellular conditions (arachidonic acid and GSP concentrations, as well as on enzyme synthesis) and on kinetic rates that differ between PTGS1 and PTGS2. The differences between PTGS1 and PTGS2 enzymes appear to show adaption to their respective roles as potent constitutively expressed or inducible enzymes. The kinetic rates appropriate for PTGS1 and PTGS2 using Scheme 1 of Lu et al. [4] (that served as a basis for the modeling reported here) were determined by Lu et al. [4] through stopped flow spectrophotometry at 4 °C, using several hydroperoxides as substrates. They reported that the k_2 and k_6 rate constants appear to differ between PTGS1 and PTGS2, leading to a faster rate of formation of Intermediate II in PTGS2. This is consistent with the difference in switching levels we found, and with their explanation of how the PTGS2 cyclooxygenase activity is activated at 10-fold lower hydroperoxide levels than required for PTGS1. They point out the potential importance of this difference in the rate of Intermediate II formation in the context of the cellular environment, and the need for combined modeling of PTGS and the GSP scavengers to represent in vivo conditions. Although, they did not identify the general switching behavior we found, our modeling reproduced the results they present. The switching behavior is most readily seen by holding the arachidonic acid concentration fixed at different levels. We did this to approximate intracellular conditions where the arachidonic acid concentration may change slowly due to its quite free diffusion between compartments and across cell membranes. The simulations of Lu et al. [4] did not assume constant arachidonic acid concentrations.

4. Discussion

Control of inherently potent agents requires an adaptable threshold for activation, a quick response proportional to the demands of the situation, and eventual inactivation of the agents. These properties are embodied in a simple autocatalytic model with threshold switching behavior that we propose (Fig. 1), where the threshold depends on model parameters and substrate concentration. The switch is quasi-linear. When substrate concentration is above threshold, output is roughly proportional to the difference between substrate concentration and threshold; output is switched off after substrate concentration drops below threshold. The threshold switching properties of this simple model have been shown to extend to a class of regulatory networks formed by insertion of short-lived intermediates at various points in the simple autocatalytic model. (The extension to a class of networks assumes that the extended models in this class are well represented by the extended Michaelis–Menten reaction scheme of the basic model.) Specific instances of this class of switches are seen in previously developed branched-chain reaction schemes for the interaction between peroxidase and cyclooxygenase activities of the PTGS1 and PTGS2 enzymes [4,10,19]. Slight differences in parameters affecting the tuning of the threshold for different isoforms appear to explain their adaption to different physiological roles as constitutive or inducible enzymes.

Regulation of PTGS1 by the network allows enzymatic control of the production of PGH_2, the precursor for a number of potent prostanoids, with arachidonic acid concentration and availability of peroxide acting as regulatory signals. Regulatory features for PTGS1 consistent with performing housekeeping functions are: (1) Abundant latent enzyme that may be immediately activated by an increased arachidonic acid signal to allow consistent response over a wide range of arachidonic acid concentrations [11]. (2) Branched chain amplification for quick response to triggering signals [3]. (3) Enzyme latency or minimal response for signal below some noise threshold. (This is especially important with branched chain amplification to avoid improper response and depletion of enzyme stores). (4) Adjustable threshold adaptable to cellular conditions. (5) Response in a physiologically useful range roughly proportional to signal intensity above threshold. (6) Eventual inactivation of activated enzyme to bring the response to an end [12,14,15]. Features (3) and (4) are identified with the threshold switching behavior shown for the first time in this paper. All of the features are embodied in the branched chain PTGS model shown in Fig. 2, based on mathematical modeling of Eq. (12) using the parameters for PTGS1 in Table 2.

Most of the features identified for PTGS1 are also useful for regulation of PTGS2. However, when induced, the low switching threshold for PTGS2, allowing PTGS2 to produce prostaglandins even at sub-micro-molar arachidonic acid concentrations, contributes to maximizing the effect of the induction signal(s). Comparison of the switching behavior of PTGS1 and PTGS2 is shown in Fig. 4. In the absence of induction, PTGS2 is not present, so there is no need for a high arachidonic acid threshold to avoid PGH2

production by arachidonic acid noise. Thus the properties of PTGS2 may reflect selection for proportional response to a broader range of arachidonic acid concentrations, arising through modifications to PTGS2 rate parameters that lower the threshold for switching.

In conclusion, the biochemical models for PTGS1 and PTGS2 are examples of a class of networks that switch on when the substrate concentration exceeds an adaptable threshold. Production of product is approximately proportional to the difference between substrate concentration and threshold. This switching behavior differs significantly between PTGS1 and PTGS2, with the higher threshold for PTGS1 consistent with the requirements for avoiding spurious activation with the constitutively expressed PTGS1. Under physiological conditions, synthesis of PTGS1 or PTGS2 allows indefinite production of prostanoids as long as synthesis continues and substrate levels remain above the threshold. We have shown through mathematical modeling how the PTGS1 and PTGS2 enzymes are adapted to their physiological roles as rapidly responding constitutive or inducible enzymes that avoid potentially damaging consequences by incorporating a switching threshold to avoid triggering by signal noise.

Acknowledgments

We thank Richard Kulmacz, Suresh Moolgavkar, and the PTGS modeling group at Fred Hutchinson Cancer Research Center for helpful discussions. This work was supported by the National Cancer Institute under grant number R01CA89445. Joe Tien was funded by an NSF Integrative Graduate Education and Research Training (IGERT) grant to Cornell University, Award #9870631.

References

[1] Kulmacz RJ, Pendleton RB, Lands WE. Interaction between peroxidase and cyclooxygenase activities in prostaglandin-endoperoxide synthase. Interpretation of reaction kinetics. J Biol Chem 1994;269(8):5527–36.
[2] Kulmacz RJ. Cellular regulation of prostaglandin H synthase catalysis. FEBS Lett 1998;430:154–7.
[3] Wei C, Kulmacz RJ, Tsai AL. Comparison of branched-chain and tightly coupled reaction mechanisms for prostaglandin H synthase. Biochemistry 1995;34:8499–512.
[4] Lu G, Tsai A-L, Van Wart HE, Kulmacz RJ. Comparison of the peroxidase reaction kinetics of prostaglandin H synthase-1 and -2. J Biol Chem 1999;274:16162–7.
[5] Smith WL, Langenbach R. Why there are two cyclooxygenases. J Clin Invest 2001;107:1491–5.
[6] Smith CJ, Zhang Y, Koboldt CM, Muhammad J, Zweifel BS, Shaffer A, et al. Pharmacological analysis of cyclooxygenase-1 in inflammation. Proc Natl Acad Sci USA 1998;95:13313–8.
[7] Taketo MM. Cyclooxygenase-2 Inhibitors in Tumorigenesis (Part II). J Natl Cancer Inst 1998;90:1609–20.
[8] Cao Y, Prescott SM. Many actions of cyclooxygenase-2 in cellular dynamics and in cancer. J Cell Physiol 2002;190:279–86.
[9] Ueno N, Murakami M, Tanioka T, Fujimori K, Tanabe T, Urade Y, Kudo I. Coupling between cyclooxygenase, terminal prostanoid synthase, and phospholipase A2. J Biol Chem 2001;276(37): 34918–27.
[10] Chen W, Pawelek T, Kulmacz RJ. Hydroperoxide dependence and cooperative cyclooxygenase kinetics in prostaglandin H synthase-1 and -2. J Biol Chem 1999;274:20301–6.
[11] Murakami M, Kambe T, Shimbara S, Kudo I. Functional coupling between various phospholipase A2s and cyclooxygenases in immediate and delayed prostanoid biosynthetic pathways. J Biol Chem 1999;274(5):3103–15.
[12] Marshall PJ, Kulmacz RJ, Lands WE. Constraints on prostaglandin biosynthesis in tissues. J Biol Chem 1987;262:3510–7.
[13] Kulmacz RJ, Wang LH. Comparison of hydroperoxide initiator requirements for the cyclooxygenase activities of prostaglandin H synthase-1 and -2. J Biol Chem 1995;270:24019–23.
[14] Smith WL, Lands WE. Oxygenation of polyunsaturated fatty acids during prostaglandin biosynthesis by sheep vesicular gland. Biochemistry 1972;11:3276–785.
[15] Wu G, Wei C, Kulmacz RJ, Osawa Y, Tsai AL. A mechanistic study of self-inactivation of the peroxidase activity in prostaglandin H synthase. J Biol Chem 1999;274:9231–7.
[16] Karthein R, Dietz R, Nastainczyk W, Ruf HH. Higher oxidation states of prostaglandin H synthase. EPR study of a transient tyrosyl radical in the enzyme during the peroxidase reaction. Eur J Biochem 1988;171(1–2):313–20.
[17] Dietz R, Nastainczyk W, Ruf HH. Higher oxidation states of prostaglandin H synthase. Rapid electronic spectroscopy detected two spectral intermediates during the peroxidase reaction with prostaglandin G2. Eur J Biochem 1988;171(1/2):321–8.
[18] Bakovic M, Dunford HB. Intimate relation between cyclooxygenase and peroxidase activities of prostaglandin H synthase. Peroxidase reaction of ferulic acid and its influence on the reaction of arachidonic acid. Biochemistry 1994;33(21):6475–82.
[19] Bambai B, Kulmacz RJ. Prostaglandin H synthase: effects of peroxidase co-substrates on cyclooxygenase velocity. J Biol Chem 2000;275:27608–14.
[20] Wu G, Vuletich JL, Kulmacz RJ, Osawa Y, Tsai AL. Peroxidase self-inactivation in prostaglandin H synthase-1 pretreated with cyclooxygenase inhibitors or substituted with mangano protoporphyrin IX. J Biol Chem 2001;276(23):19879–88.
[21] Swinney DC, Mak AY, Barnett J, Ramesha CS. Differential allosteric regulation of prostaglandin H synthase 1 and 2 by arachidonic acid. J Biol Chem 1997;272(19):12393–8.
[22] Tsai A, Wu G, Palmer G, Bambai B, Koehn JA, Marshall PJ, et al. Rapid kinetics of tyrosyl radical formation and heme redox state changes in prostaglandin H synthase-1 and -2. J Biol Chem 1999;274(31):21695–700.
[23] Tsai A, Palmer G, Xiao G, Swinney DC, Kulmacz RJ. Structural characterization of arachidonyl radicals formed by prostaglandin H synthase-2 and prostaglandin H synthase-1 reconstituted with mangano protoporphyrin IX. J Biol Chem 1998;273(7): 3888–94.
[24] Tsai A, Kulmacz RJ. Tyrosyl radicals in prostaglandin H synthase-1 and -2. Prostaglandins Other Lipid Mediators 2000;62(3):231–54.
[25] Edelstein-Keshet L. Mathematical models in biology. Birkhauser mathematics series. Random House; 1988.
[26] Fersht A. Structure and mechanism in protein science: a guide to enzyme catalysis and protein folding. W.H. Freeman Co.; 1999.
[27] Segel LA, Slemrod M. The quasi-steady-state assumption: a case study in perturbation. SIAM Rev 1989;31:446–77.